AD-A117 589 NAVAL POSTGRADUATE SCHOOL MONTEREY CA F/G 11/6
THERMAL MARTENSITIC TRANSFORMATION CYCLING IN CU-ZN-AL SHAPE ME--ETC(U)
MAR 82 W E MUESING

UNCLASSIFIED

NL

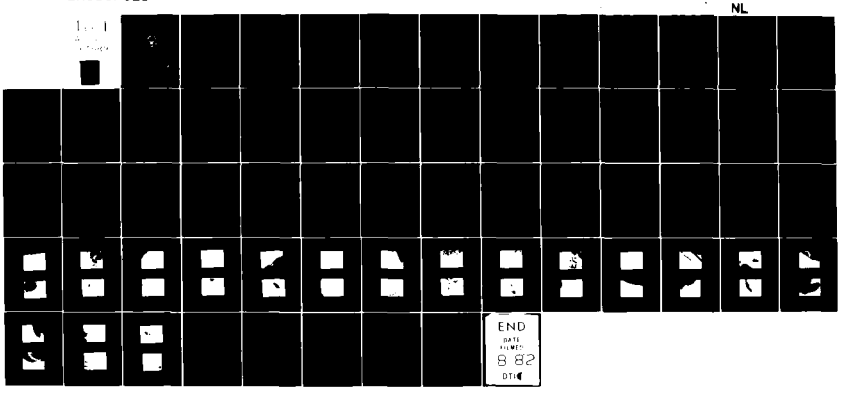

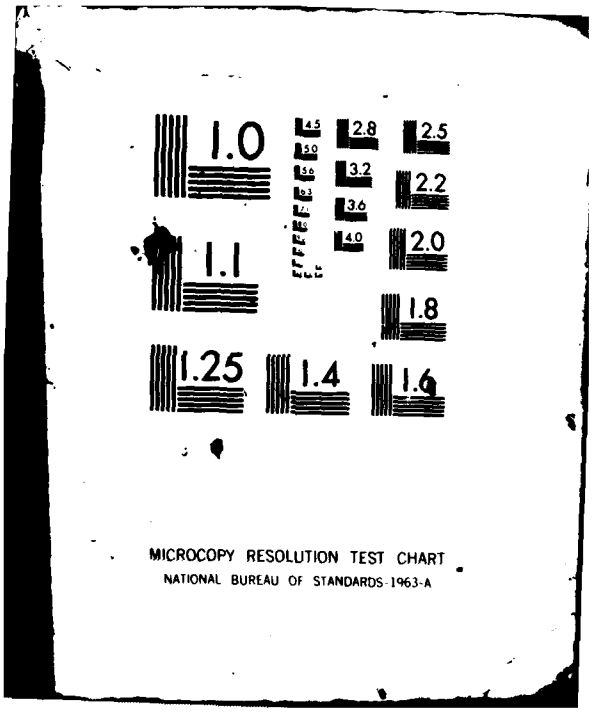
1.0
1.1
1.25
1.4
1.6
1.8
2.0
2.2
2.5
2.8
3.2
3.6
4.0
4.5
5.0
5.6
MICROCOPY RESOLUTION TEST CHART
NATIONAL BUREAU OF STANDARDS-1963-A

NAVAL POSTGRADUATE SCHOOL
Monterey, California

THESIS

THERMAL MARTENSITIC TRANSFORMATION
CYCLING IN Cu-Zn-Al SHAPE MEMORY ALLOYS

by

William E. Muesing

March 1982

Thesis Advisor: A. J. Perkins

Approved for public release; distribution unlimited.

SECURITY CLASSIFICATION OF THIS PAGE (When Data Entered)

REPORT DOCUMENTATION PAGE	READ INSTRUCTIONS BEFORE COMPLETING FORM
1. REPORT NUMBER	2. GOVT ACCESSION NO. AD-A117589	3. RECIPIENT'S CATALOG NUMBER
4. TITLE (and Subtitle) Thermal Martensitic Transformation Cycling in Cu-Zn-Al Shape Memory Alloys	5. TYPE OF REPORT & PERIOD COVERED Master's Thesis; March 1982
	6. PERFORMING ORG. REPORT NUMBER
7. AUTHOR(s) William E. Muesing	8. CONTRACT OR GRANT NUMBER(s)
9. PERFORMING ORGANIZATION NAME AND ADDRESS Naval Postgraduate School Monterey, California 93940	10. PROGRAM ELEMENT, PROJECT, TASK AREA & WORK UNIT NUMBERS
11. CONTROLLING OFFICE NAME AND ADDRESS Naval Postgraduate School Monterey, California 93940	12. REPORT DATE March 1982
	13. NUMBER OF PAGES 61
14. MONITORING AGENCY NAME & ADDRESS(if different from Controlling Office)	15. SECURITY CLASS. (of this report) Unclassified
	15a. DECLASSIFICATION/DOWNGRADING SCHEDULE

16. DISTRIBUTION STATEMENT (of this Report)

Approved for public release; distribution unlimited.

17. DISTRIBUTION STATEMENT (of the abstract entered in Block 20, if different from Report)

18. SUPPLEMENTARY NOTES

19. KEY WORDS (Continue on reverse side if necessary and identify by block number)

Martensite
Transformation

20. ABSTRACT (Continue on reverse side if necessary and identify by block number)

The effect of multiple thermal cycles between the martensitic phase and parent phase of selected Cu-Zn-Al alloys was studied. As thermal cycling progressed the martensite start temperature (M_s), parent phase finish temperature (A_f), and the temperature at which the maximum martensitic peak height occurred (M_{max}) were all observed to shift upward. The proportion of the sample undergoing thermal transformation decreased with increasing

DD FORM 1 JAN 73 1473 EDITION OF 1 NOV 65 IS OBSOLETE
S/N 0102-014-6601

SECURITY CLASSIFICATION OF THIS PAGE (When Data Entered)

numbers of thermal cycles, as was noted by a decrease of total transformation energy. Examination in a transmission electron microscope found dislocation substructures apparently generated by the martensitic transformations.

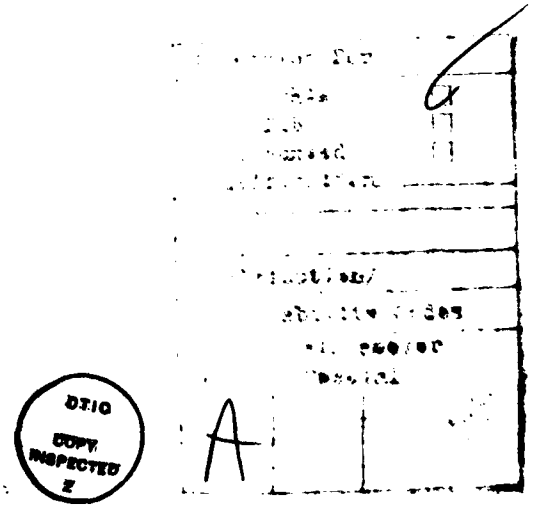

Approved for public release; distribution unlimited.

Thermal Martensitic Transformation Cycling
in Cu-Zn-Al Shape Memory Alloys

by

William E. Muesing
Lieutenant, United States Navy
B.S., United States Naval Academy, 1974

Submitted in partial fulfillment of the
requirements for the degree of

MASTER OF SCIENCE IN MECHANICAL ENGINEERING

from the

NAVAL POSTGRADUATE SCHOOL
March 1982

Author: William E. Muesing

Approved by: Jeff Perkins
Thesis Advisor

Kenneth D. Challenger
Second Reader

P. J. Marto
Chairman, Department of Mechanical Engineering

William M. Tolles
Dean of Science and Engineering

ABSTRACT

The effect of multiple thermal cycles between the martensitic phase and parent phase of selected Cu-Zn-Al alloys was studied. As thermal cycling progressed the martensite start temperature (M_s), parent phase finish temperature (A_f), and the temperature at which the maximum martensitic peak height occurred (M_{max}) were all observed to shift upward. The proportion of the sample undergoing thermal transformation decreased with increasing numbers of thermal cycles, as was noted by a decrease of total transformation energy. Examination in a transmission electron microscope found dislocation substructures apparently generated by the martensitic transformations.

TABLE OF CONTENTS

LIST OF TABLES

LIST OF FIGURES

LIST OF MICROGRAPHS

I. INTRODUCTION

Certain alloys have the unusual ability to recover an original shape after undergoing what would appear to be permanent deformation. These are the so-called Shape Memory Alloys and the property of assuming a former shape is known as Shape Memory Effect (SME). As the shape memory alloy is reverting back to a previous shape, a large force is exerted. Proper development of these alloys and harnessing of this force is offering a new approach to thermally activated controls. Variable orifice jets for automobile carburetors, fluid and gas control valves, thermally operated relays and switches, thermostatic valves, and even heat engines are several possible uses now being studied for shape memory alloys. In the field of medicine there appear to be many applications for these alloys, reliant on their ability to change shape after installation and subsequent warming by the body.

The shape memory effect is a direct result of thermoelastic martensitic transformation. Unlike other alloys such as steels which undergo martensitic transformations, the shape memory alloy transforms to martensite by forming plates which continue to grow in a continuous manner as temperature is decreased, and as the temperature is raised the plates revert back to the parent phase in an exact reverse path of

the original transformation [Ref. 1]. In most shape memory alloys, there is only one crystallographic route back to the parent phase, while there are several thermal or stress related routes to induce or deform the martensite. So, when one of these alloys is deformed while martensitic, it will regain its original shape as the temperature is raised above that necessary for complete phase transformation to the parent phase (A_f). The ability to regain the original shape is due to the nearly exact reconstruction of the original parent crystal, on an atomic level.

Among the shape memory alloys with greatest potential for practical applications, are the Copper-Zinc-Aluminum alloys. The Cu-Zn-Al shape memory alloys are typically about 70 wt.% copper brasses with some aluminum, and the reaction of importance is the transformation of the ordered body centered cubic (BCC) beta phase to a close packed thermoelastic martensitic structure. The Cu-Zn-Al alloys have several advantages over other shape memory materials such as i) relatively low cost, ii) ease of fabrication, and iii) availability of a useful range of martensite transformation temperatures (achieved by slight variations of alloy composition).

The predominant form of thermally induced martensite in the Cu-Zn-Al alloys is the β', an orthorhombic 9R or 18R variant with ABCBCACAB/A stacking sequence. The transformation from the body centered cubic structure is a diffusionless one in which the martensite inherits the long range

order of the parent phase. The stresses accompanying the transformation do not produce significant plastic deformation or disrupt the continuity between the martensite and parent lattice. As the martensite plates grow, self-accommodation takes place by faulting, resulting in very low elastic strains, i.e., strains not exceeding the elastic limit of the parent lattice.

Deformation of a martensitic Cu-Zn-Al shape memory alloy causes growth, shrinkage and shifting of martensitic plates to an orientation favorable to the applied stress. Some of these alloys have shape memory properties even above M_s. When strained, stress induced martensite forms from the beta matrix and this stress induced martensite has the same characteristics as the athermal martensite. A lowering of temperature or the application of stress produces the same effect in terms of inducing formations of martensite, while raising the temperature or relieving stress both tend to recreated the parent phase. The key is that martensite may be induced or deformed (to a limit) without destroying the continuity with the parent lattice.

The purpose of this study was to observe the results of multiple thermal cycles between the beta parent (A) and martensitic (M) phases of selected Cu-Zn-Al alloys. By using a differential scanning calorimeter, specific temperatures, which are the milestones of the transformation process, can be recorded during thermal cycling. Thus, slight changes in

the transformation character may be detected as shifts of these temperature milestones, and a study of these shifts coupled with transmission electron microscope observations is intended to lead to better understanding the mechanisms of thermoelastic martensitic transformations.

II. EXPERIMENTAL PROCEDURES

A. SAMPLE PREPARATION

The Cu-Zn-Al alloys studied were provided by Delta Materials Research Limited, Ipswich, Suffolk, England. Nominal compositions and reputed M_s temperatures are given in Table I. These alloys were chosen on the basis of M_s temperatures; alloy D reputedly existing as the β parent phase at room temperature and alloy E as martensite. The as-received alloys were cut into disks of 3mm diameter and .25 - .40mm thickness. To homogenize and eliminate second phase precipitates while minimizing zinc loss, the samples were sealed in evacuated quartz tubes and annealed at 900°C for 15 minutes. Quenching was accomplished by shattering the quartz tubes in cold water immediately upon removal from the furnace. The resulting grain size in both alloys was large; about .3mm diameter. After annealing, alloy D was observed to have a homogeneous microstructure, consisting entirely of the parent phase. Alloy E appeared to be nearly all martensitic.

Table I. Experimental Alloys (at %)

Alloy	Cu	Zn	Al	Reputed M_s
D	66.2	24.8	9.0	263°K
E	68.4	18.6	13.0	323°K

B. DIFFERENTIAL SCANNING CALORIMETRY

To characterize the martensitic transformation during thermal cycling, a differential scanning calorimeter (Perkin Elmer DSC-2) was utilized. The DSC measures changes in power required to maintain sample and sample holder at the same temperature as a reference holder. Transformation from the beta phase to martensite is exothermic while the reverse transformation, from martensite back to the parent structure, is endothermic. Start and finish temperatures of these reactions are recorded on the chart abscissa. The area under the generated curves is a quantitative measure of the energy transferred to or from the sample, and therefore is directly related to the amount of material undergoing transformation. For alloy D, the DSC was programmed to cycle from 240°K to 300°K, at least 10°K above A_f and below M_f. Alloy E was cycled between 260°K and 340°K. A slow heating-cooling rate of 10°K per minute was chosen to ensure thorough transformation during the temperature excursions and to allow easy data reduction from the strip chart recordings.

M_{max} and A_{max} were defined as the peak temperatures, determined as the temperatures where the maximum transformation rate occurred (maximum displacement on the ordinate in mcal./sec from the alloys' predetermined baselines). M_s and A_s were chosen as the temperatures corresponding to the points where the generated curves departed from the pretransformed baselines, while M_f and A_f corresponded to the beginning of

the past transformation baseline (Fig. 1a). Measurement of area under these peaks was difficult because the parent phase and transformed martensite have different specific heats and therefore different baselines. The area was estimated as being bordered by the curve and a line connecting the start and finish transformation temperatures (Fig. 1b). Partial thermal cycling was accomplished between the approximate M_{max} and A_{max} temperatures, as determined by an initial complete thermal cycle (above A_s to below M_f, and back to above A_f). Transformation peak width was measured at one half the peak height. Polynomial curve fits were generated to better define the shifts of the studied characteristic temperatures. A_{max} and M_{max} (Fig. 2), A_f (Fig. 3), M_f and A_s (Fig. 4), A_{width} (Fig. 8), $A_{max} - M_{max}$ (Fig. 7), and A_{height} (Fig. 9) are third order polynomial curves. M_s (Fig. 3) is a forth order while M_{area} and A_{area} (Figs. 5 and 6), M_{width} (Fig. 8) and M_{height} (Fig. 9) are all second order.

C. TRANSMISSION ELECTRON MICROSCOPY

The disks were prepared by electropolishing in a 10% KCN solution using 12-18 volts A.C. at room temperature. The finished foils were examined and photographed with a Japan Electron Optics Lab Co., LTD. Transmission Electron Microscope, Model JEM-7. Foils of both alloys were studied prior to and after twenty complete thermal cycles in the DSC, with the goal of observing changes in microstructure that might help to characterize the transformation process.

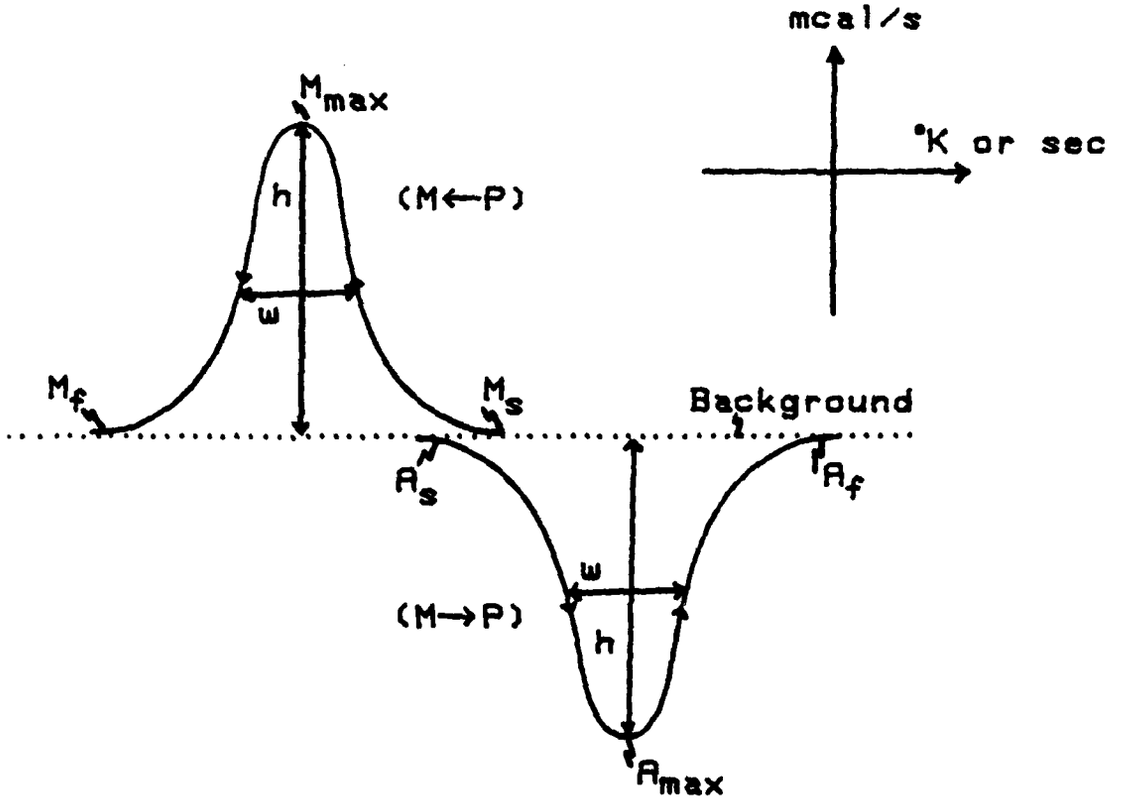

Figure 1a. Example of the determination of M_s, M_f, M_{max}, A_s, A_f, A_{max}, h (peak height), and w (peak width).

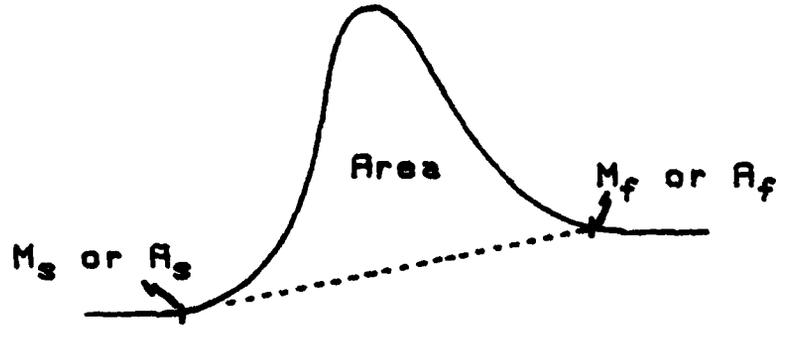

Figure 1b. Estimated area used for the determination of the energy of transformation.

III. RESULTS AND DISCUSSION

A. DIFFERENTIAL SCANNING CALORIMETRY

Much of the data from this study indicates that multiple thermal transformation cycling establishes favored nucleation sites for the martensitic transformation and stabilizes the martensite. For example, M_{max}, the temperature at which the greatest quantity of material is undergoing transformation, is seen to shift upward as the number of thermal cycles increases. This is consistent with the establishment of a set of preferred nucleation sites as cycling progresses. As these preferred sites are "learned," martensite nucleates and forms more readily, and M_{max} creeps upward. Pops and Massalski [Ref. 2] found that martensitic transformations in Cu-Zn beta phase alloys have two stages, a thermoelastic stage and a "burst" type. The occurrence of the "burst" martensite diminishes and vanishes altogether during multiple thermal cycling. Pops and Massalski have also shown that the formation of "burst" martensite produces lattice defects and some degree of plastic deformation in the parent lattice, and Kajiwara [Ref. 3] has found that thermal cycling introduces dislocations into the matrix phase. Guenin and Gobin [Ref. 4] postulated that zones of instability exist around dislocations and these regions may play an important role in the nucleation of martensite. It is therefore likely

that as cycling progresses, debris from multiple transformations accumulates, and this debris provides more of the preferred martensite nucleation sites. A corresponding decrease of A_{max} is not observed because, whereas the parent phase to martensite reaction depends on nucleation, the reverse martensite to parent phase reaction does not; the reversion simply involves shrinkage of the martensite crystalites back to the parent phase. Accompanying the shifting relative values of M_{max} and A_{max} is a shrinking of the A_{max} - M_{max} hysteresis (Fig. 7). The bulk of the martensite is obviously stable at temperatures above M_{max} of the first transition. As nucleation occurs at higher temperatures, the martensitic growth also moves to higher temperatures.

Stabilization of the martensite is evidenced by the tendency of the M_s and A_f temperatures to rise with cycling (Fig. 3). Martensite nucleates and grows at higher temperatures during cooling, and around these same nucleation sites it remains to higher temperatures during heating. The increasing width of the martensite and parent phase peaks (Fig. 8) is related to the M_s and A_f shifts. All of these factors indicate that the martensite is able to exist over a wider range of temperatures and therefore, thermal cycling has a stabilizing effect on the martensite relative to the parent phase.

As the number of complete thermal cycles increases, it is seen that the amount of transformation taking place during both the cooling and heating cycles decreases (Fig. 6,7).

There are two possible explanations for this noted reduction. The first possibility is that the transformations have become more spread out and the last bits of each transformation are incorporated with the base line and therefore not detected in our data reduction process. This explanation is supported by the general increasing stability of the martensitic phase at higher temperatures. A second and more probable explanation is that less material undergoes transformation after multiple thermal cycles. Either some martensite is retained (on heating above A_f) or some parent phase remains after transformation. Li and Ansell [Ref. 5], using electrical resistivity measurements, concluded that it is martensite that is retained as cycling progresses. This would mean that some martensite has become stable, at least within the temperature ranges being used, or else a "blocking structure or force develops which prevents the martensite from transforming back to the parent phase even at temperatures above A_f. Whichever is the explanation, it is clear that the transformation, especially during the first few cycles, is not a completely reversible process. Some degree of irreversible behavior is taking place and is represented by the decreasing total energy of transformation. Eventually a limit is reached where the total transformation energy remains constant with continued cycling. Further cycles are more completely reversible in nature, that is with a given cycle having the same amount of transformation as the preceding cycle.

During thermal cycling, structures such as secondary peaks develop on the primary peaks. As more thermal cycles are completed, these structures smooth out and eventually blend back into the primary peak. This occurrence is probably not due to "burst" martensite but to a more macroscopic smoothing out of the transformation kinetics. An analogy could be made to creating a trail through initially virgin underbrush. The first time the path is taken travel is difficult. But, upon using the route several times, the trail is more and more established until eventually steady progress is made while traveling it, and no further significant improvements in the trail are possible.

Partial thermal cycling between (approximately) the A_{max} and M_{max} temperatures demonstrated that the proportion of material not transforming during the partial cycles would, upon completion of partial cycling, transform at a different temperature than the previously active material (Table II, III). Secondary peaks occurred approximately $5^{o}K$ higher than the primary A_{max} peak and $5^{o}K$ lower than the primary M_{max} peak. Some of the alloy evidently had not "learned" the preferred nucleation sites or the transforming material was creating stresses or substructures that retarded the transformation of the rest of the metal.

To examine both of these theories, a sample, after undergoing partial thermal cycling, was then cycled ten complete times. Partial cycling was again accomplished and once more

Table II. Partial Cycling Experiment 1

ONE COMPLETE CYCLE (A_f to M_f to A_f)

M_{max}	A_{max}
261.8°K	274.6°K

40 PARTIAL CYCLES (M_{max} to A_{max} to M_{max})
FOLLOWED BY COOLING FROM A_{max} TO BELOW M_f

2 M PEAKS

$M_{max\ 1}$	$A_{max\ 2}$
266.5°K	261.2°K

HEATING TO ABOVE A_f

2 A PEAKS

$A_{max\ 1}$	$A_{max\ 2}$
275.1°K	281.0°K

COOLING BELOW M_f

1 M PEAK

M_{max}
265.5°K

Table II. (Cont'd)

HEATING ABOVE A_f

1 A PEAK

A_{max}
275.8°K

10 COMPLETE THERMAL CYCLES

$M_{max\ 10}$	$A_{max\ 10}$
266.0°K	276.5°K

40 PARTIAL CYCLES FOLLOWED BY COOLING FROM A_{max} TO BELOW M_f

2 M PEAKS

$M_{max\ 1}$	$M_{max\ 2}$
267.1°K	264.2°K

HEATING ABOVE A_f

2 A PEAKS

$A_{max\ 1}$	$A_{max\ 2}$
276.2°K	281.6°K

Table II. (Cont'd)

COOLING BELOW M_f

1 M PEAK

M_{max}

$266.1^{o}K$

HEATING ABOVE A_f

1 A PEAK

A_{max}

$276.5^{o}K$

Table III. Partial Thermal Cycling Experiment 2

ONE COMPLETE CYCLE

M_{max}	A_{max}
262.0°K	273.9°K

40 PARTIAL CYCLES FOLLOWED BY HEATING TO ABOVE A_f

2 A PEAKS

$A_{max\ 1}$	$A_{max\ 2}$
273.9°K	275.4°K

COOLING BELOW M_f

1 M PEAK

M_{max}
262.8°K

HEATING ABOVE A_f

1 A PEAK

A_{max}
273.7°K

sets of two peaks resulted. Any preferred nucleation sites or transformation paths "learned" from the complete thermal cycling were lost or forgotten as partial cycling commenced. This suggests that the latter idea of some type of inhibitor to the transformation is developing during the cycling. It is also interesting to note that if, after partial cycling the sample is directly heated above A_f, all memory of the secondary peaks in the cooling martensitic transformation and also in the heating, parent phase transformation, is lost. The same is not true if the sample is directly cooled to below M_f after partial cycling; in this case two peaks will still develop when heating to above A_f. This indicates that when the parent lattice is reconstructed during the first full heating cycle after partial cycling, it so resembles the original patent lattice that whatever caused the secondary peaks to develop has been eliminated. Secondary peaks can only be regenerated with further partial cycling.

To briefly examine the effects of cold working the beta phase brass on transformation cycling, several disks of alloy D were reduced 10%, i.e., rolled to approximately 90% of their original thickness. No response whatsoever was observed during thermal cycling within the original temperature limits ($240^{o}K$ - $300^{o}K$) or even at temperatures up to $600^{o}K$. It has been noted [Ref. 6] the plastic deformation of beta phase brass can lower the M_s up to $50^{o}K$. If this was the case, the transformation peaks may have been below the lower temperature

limit used and naturally, no peaks were generated. Examination of the deformed specimens in the TEM found that the resulting microstructure after the massive deformation contained a great deal of martensite. If the martensite was reverting back to the parent phase during heating cycles, the transformation was so spread out it cannot be distinguished from the DSC baseline. It appeared, however, from lack of evidence to the contrary, that the martensite was locked in and retained during cycling. Whether the parent phase is retained or undergoes transformation at low temperatures was not determined.

B. TRANSMISSION ELECTRON MICROSCOPY

Uncycled samples of alloy D consist, for the most part, of the homogeneous parent phase at room temperature, with low dislocation density (Micrographs 1,2). Delaey, Perkins, and Massalski [Ref. 7] have concluded the mottling or tweed like appearance, observed frequently here in both cycled and uncycled specimens, is due to a very fine precipitate and resulting surface-etch pitting during electropolishing. Scattered martensitic plates, probably formed during electropolishing, were also observed in the uncycled parent phase. Micrograph 3 reveals a number of martensite plates on different habit plane variants, interacting at an early stage of growth. In Micrograph 4, a subtle change in habit plane is noted at a very early stage of growth. Martensite

plates appear to be developing in association with an array of imperfections in Micrograph 5. This situation may constitute the preferred nucleation site model discussed previously.

The most interesting feature observed in the thermally cycled D alloys were the abundance of dislocations and dislocation tangles (Micrographs 6-10). These photo-micrographs tend to confirm that dislocations are generated during thermal cycling. A higher dislocation density brings about more dislocation interactions and local lattice strains associated with the observed tangles and groupings. These dislocations constitute irreversible features introduced by the thermal cycling process. It is speculated here that these dislocation structures or their resulting strain fields may be responsible for the noticeable incomplete transformation occurring after cycling, functioning either to stabilize a phase or block its transformation.

In some cases (Micrographs 11-13) we find dislocations arrayed on parallel slip planes. New martensite plates are also observed to occasionally pair up on parallel planes (Micrograph 14).

The cold worked parent phase is a complex collection of phases and debris (Micrographs 15-21). It would be expected that this alloy would be entirely parent phase but it is seen that extensive amounts of martensite are interspersed with the parent structure. Large numbers of dislocations and

other remnants from the plastic deformation are present in both the parent and martensite lattices. As was stated earlier, no transformation peaks are observed for these specimens. Something is inhibiting the regular thermal transformation of this alloy. High densities of dislocations are common to the strained alloy and the thermally cycled alloyed.

Uncycled alloy E was largely martensite as expected but did contain regions of parent phase (Micrographs 22-25). This is expected since both M_s and M_f, and A_s and A_f bracket room temperature. Dislocations (Micrograph 22) and faulting (Micrograph 23) were noted in the martensite microstructure. Few dissimilarities between the thermally cycled and uncycled alloy E were observed (Micrographs 26-30). If complete thermal cycling had occurred, it would be reasonable to expect dislocation tangles to be present as observed in alloy D, but few were found. It is therefore probable that much of alloy E is not transforming during thermal cycling. This would confirm the exceptionally small peaks generated by the DSC during cycling. No explanation is offered for this phenomenon.

IV. CONCLUSIONS

As a result of multiple thermal cycles, M_s, A_f, and M_{max} all rise. This is due to the development of preferred sites for the nucleation of martensite and or the stabilization of martensite at higher temperatures. In addition, the energy of transformation decreases as the number of completed cycles increases, indicating that less of the material undergoes transformation. This is most likely due to the retention of martensite above A_f. Partial thermal cycling accomplished between A_{max} and M_{max} produces two M peaks or A peaks, demonstrating that the proportion of the sample not transforming either does not "learn" the preferred nucleation sites and so does not stabilize that proportion of the martensite at higher temperatures, or more likely its reaction is inhibited by obstacles created by the transforming material. In either case the obstacles disappear after heating above A_f. Transmission electron microscopy reveals irreversibilities in the forms of dislocations and dislocation structures. These dislocations may in some way be connected with the specified temperature shifts and decreasing transformation energy. The transformation becomes more completely reversible from cycle to cycle as thermal cycling progresses.

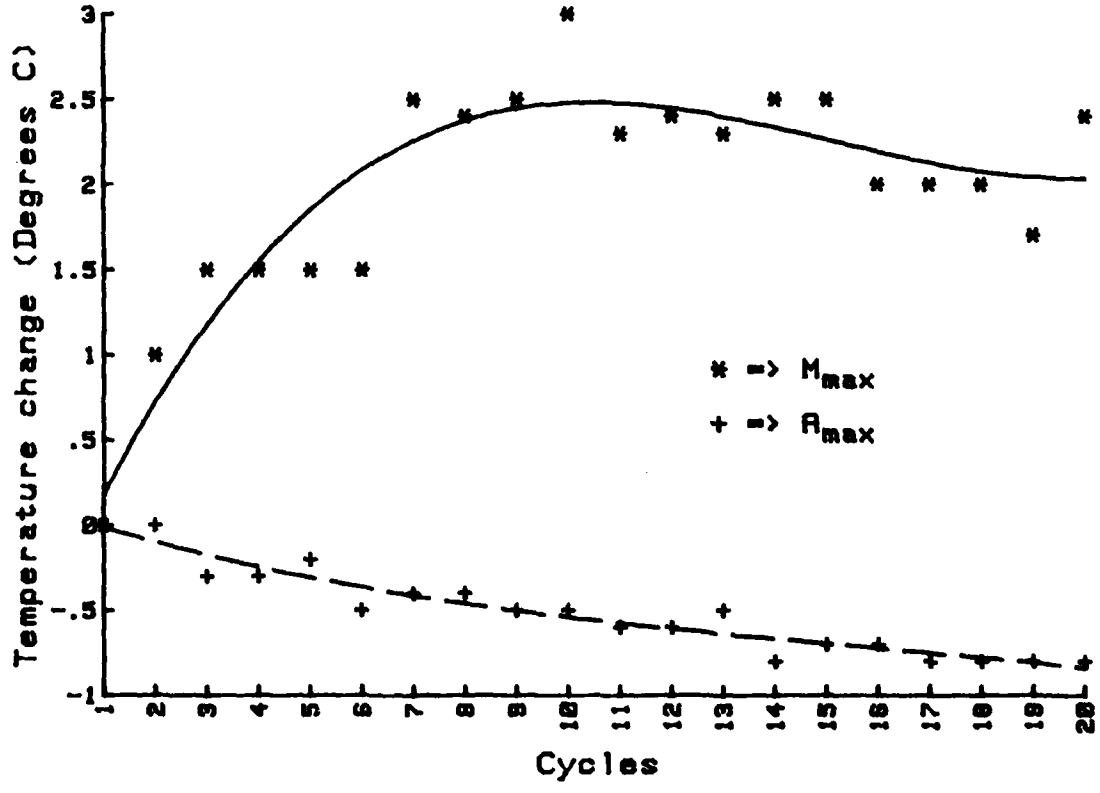

Figure 2. Shifting of the M and A temperatures at which maximum transformation is occurring (M_{max} and A_{max}) relative to the corresponding temperatures of the first complete thermal cycle, vs. the number of completed thermal cycles.

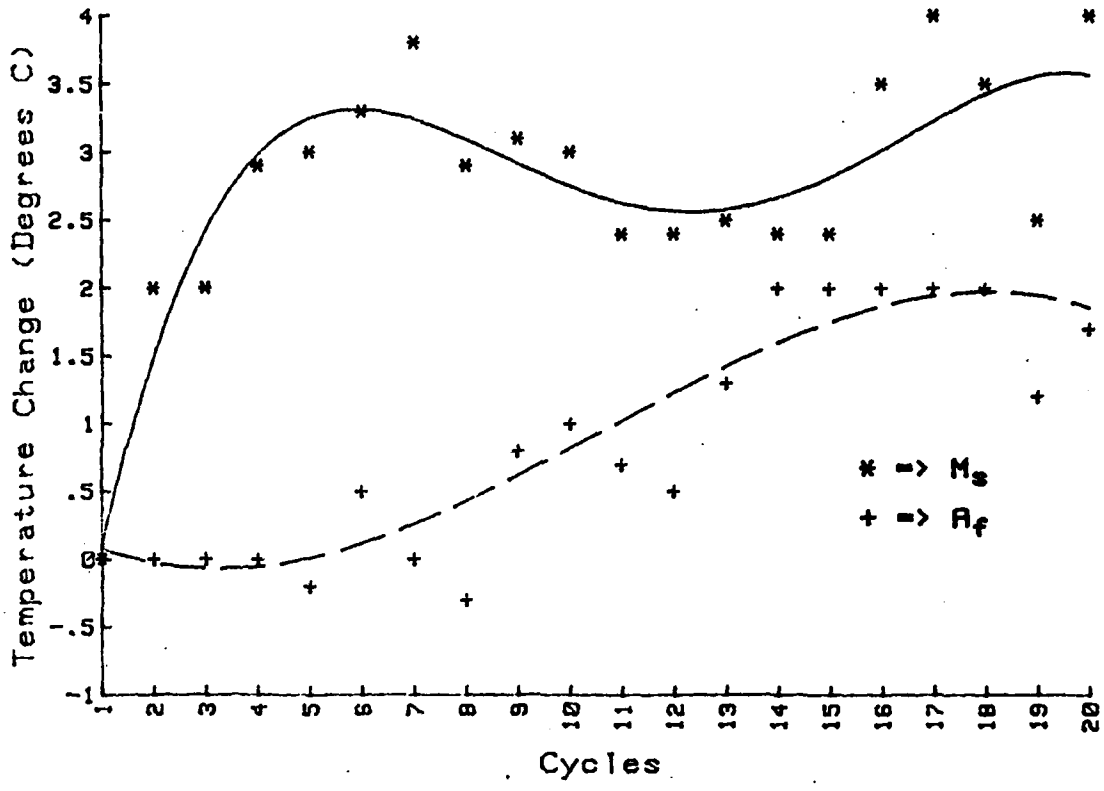

Figure 3. Shifting of the martensite start temperature (M_s) and the parent phase finish temperature (A_f) relative to the corresponding temperatures of the first thermal cycle, vs. the number of completed thermal cycles.

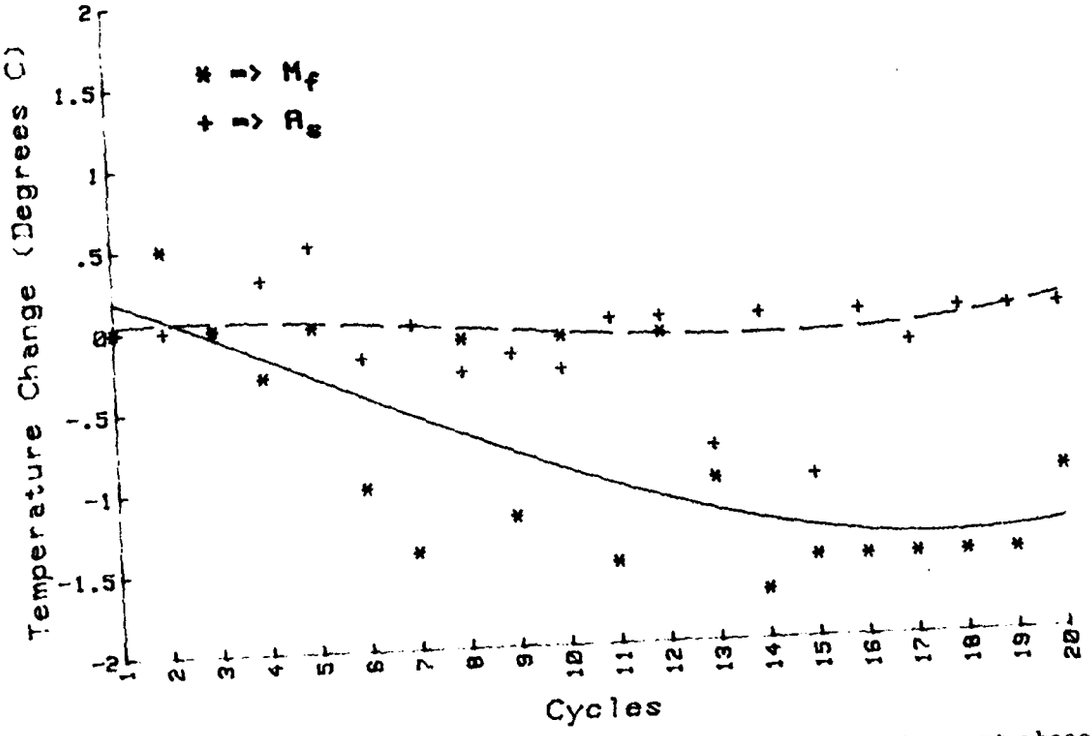

Figure 4. Values of the martensite finish temperature (M_f) and parent phase start temperatures (A_S), relative to the corresponding temperatures of the first thermal cycle, vs. the number of completed thermal cycles.

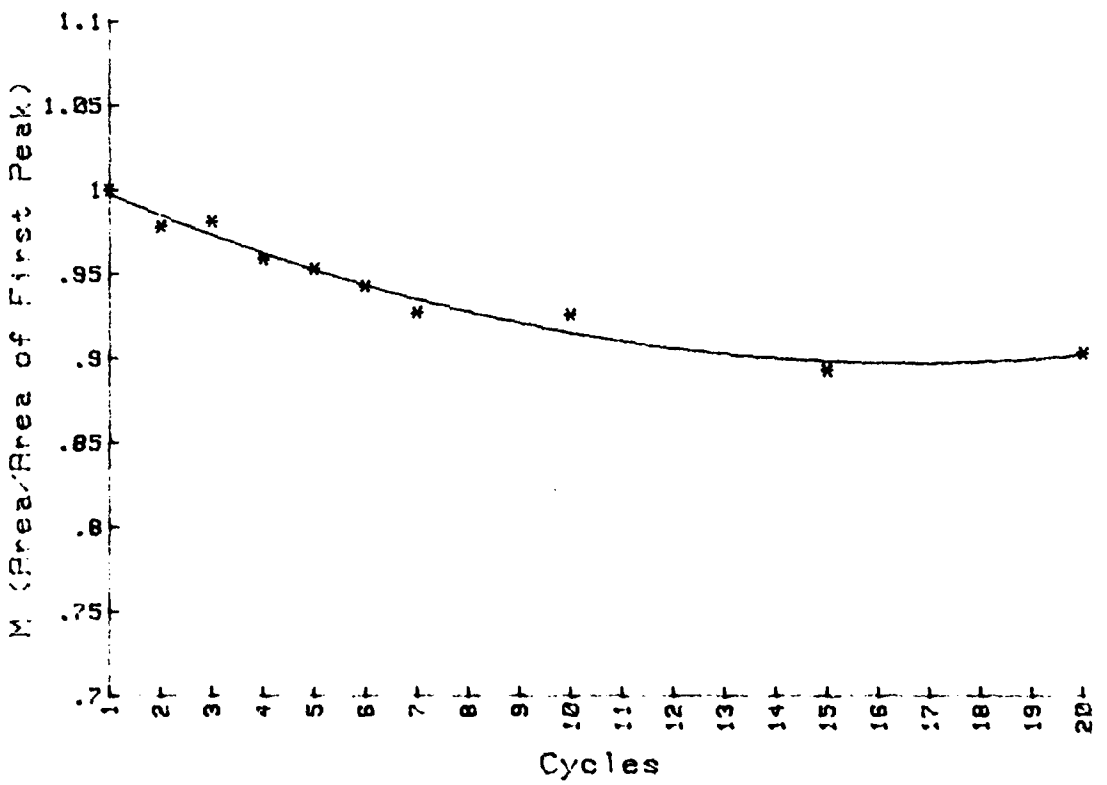

Figure 5. Energy of transformation (represented by area) of the parent phase to martensite reaction divided by that of the first cooling cycle peak, vs. the number of completed thermal cycles.

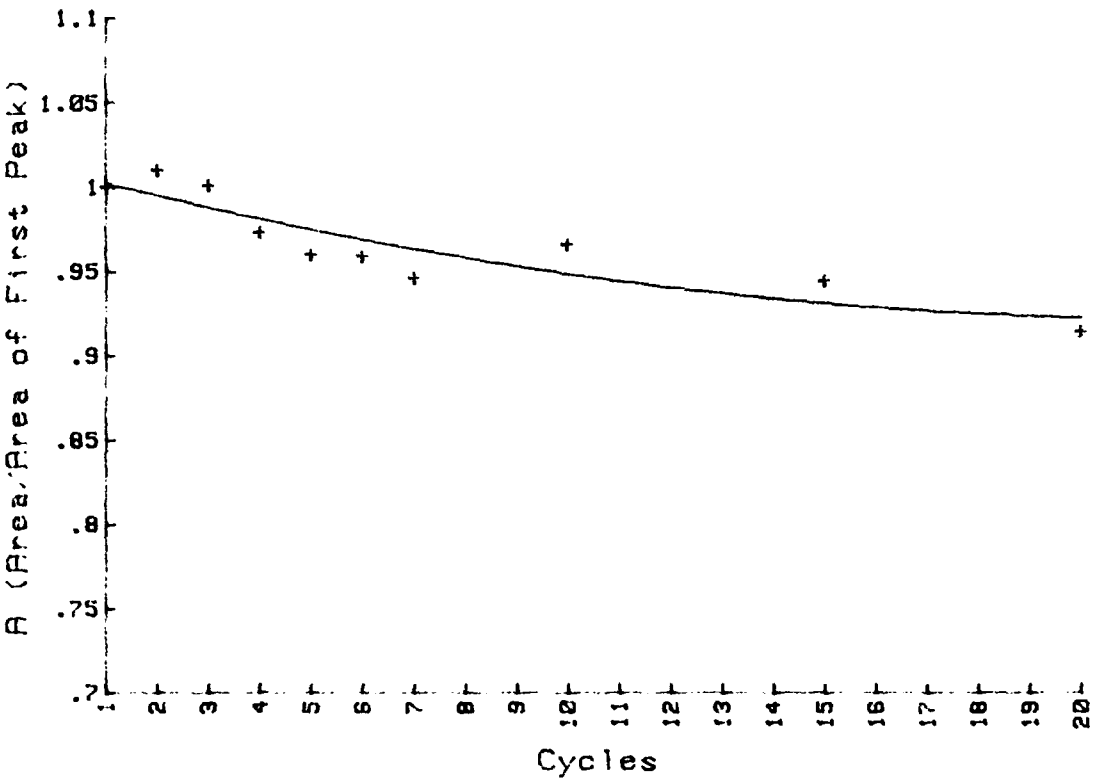

Figure 6. Energy of transformation (represented by area) of the martensite to parent phase reaction divided by that of the first heating cycle, vs. the number of completed thermal cycles.

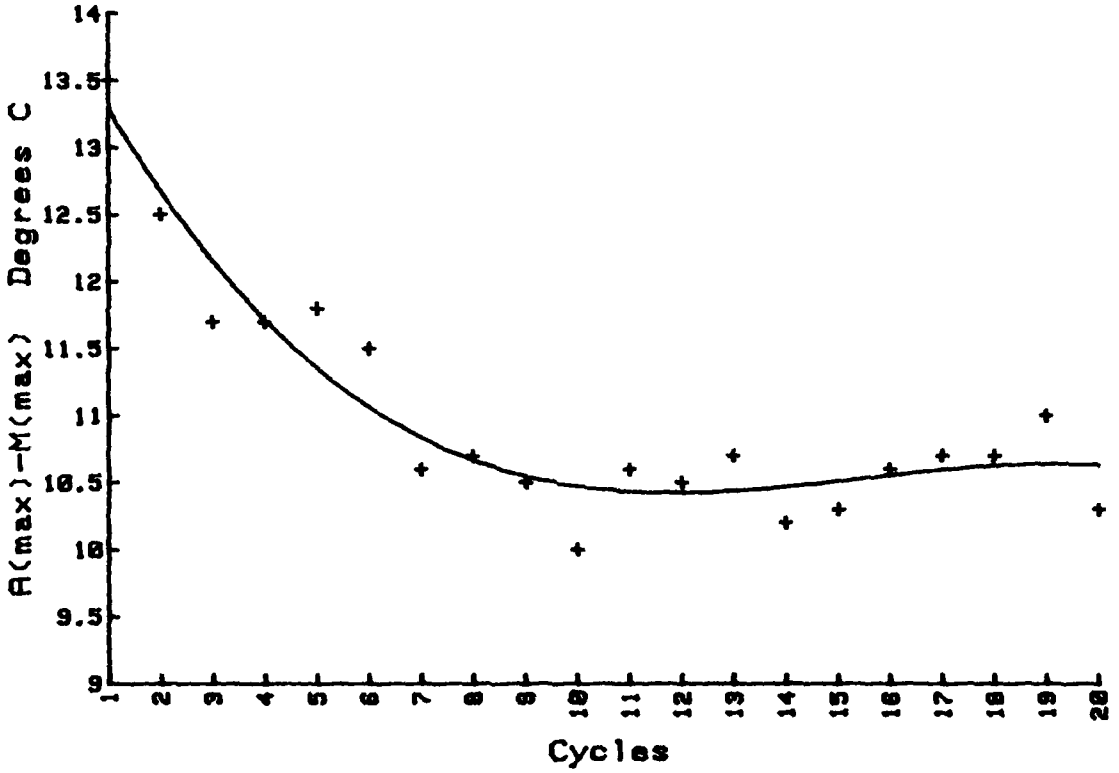

Figure 7. Difference between the transformation peak temperatures (A_{max} - M_{max}) vs. the number of completed thermal cycles.

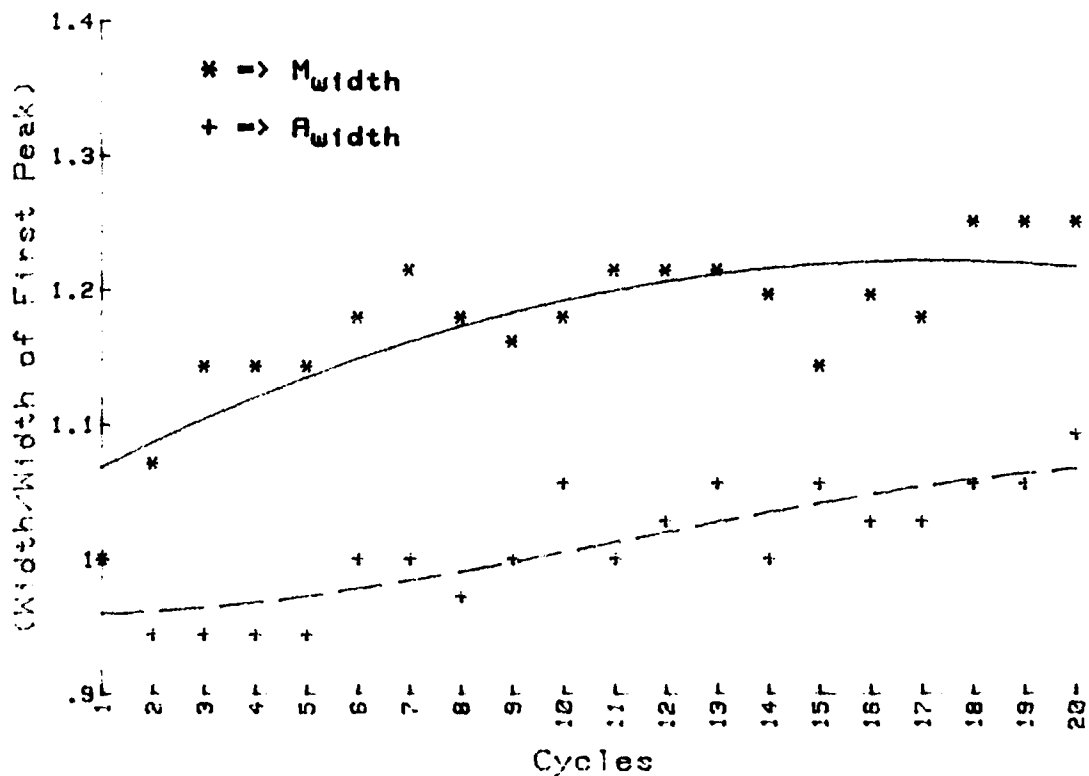

Figure 8. Value of the M and A peak widths, divided by the corresponding measured widths of the first transformation peaks, vs. the number of completed thermal cycles.

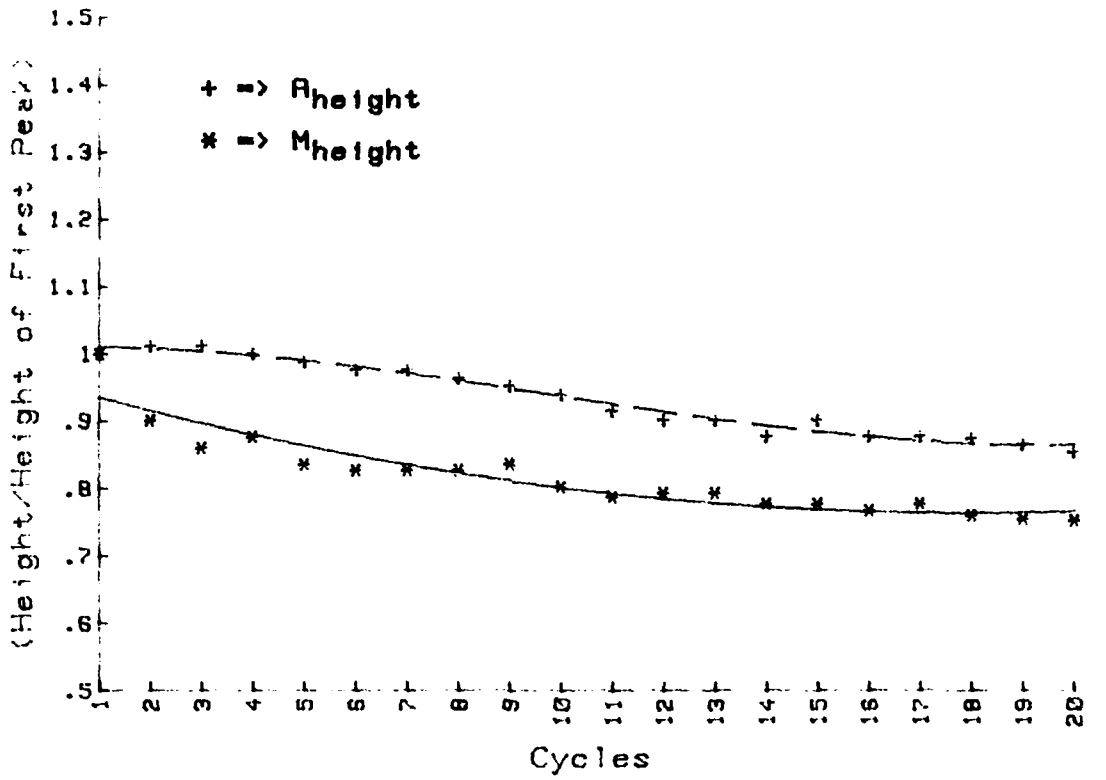

Figure 9. Values of the M and A peak heights, divided by the corresponding measured heights of the first transformation peaks, vs. the number of completed thermal cycles.

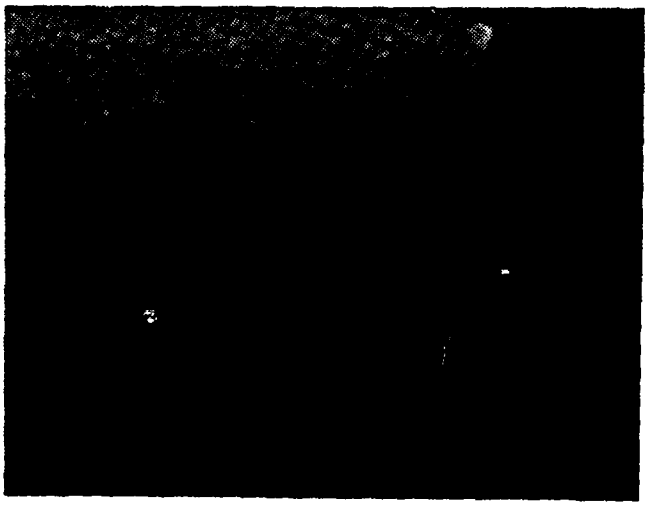

Micrograph 1. Alloy D annealed and quenched, prior to thermal cycling. The mottling observed in the beta phase is a result of selected etching during electropolishing caused by a very fine precipitate. x22,000

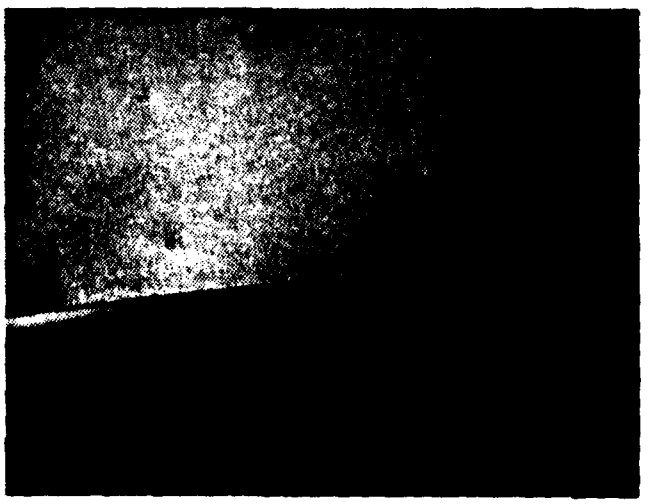

Micrograph 2. Alloy D annealed and quenched, prior to thermal cycling. The tweed-like pattern observed in Micrograph 1 is in contrast in only one of the two grains separated by a grain boundary. Note the dislocation density appears to be low in these precycled specimens. x12,500

Micrograph 3. Alloy D. The martensite plates observed here are generated by the electropolishing treatment. The martensite plate seen near the pointer may be changing habit planes after considerable growth. x10,000

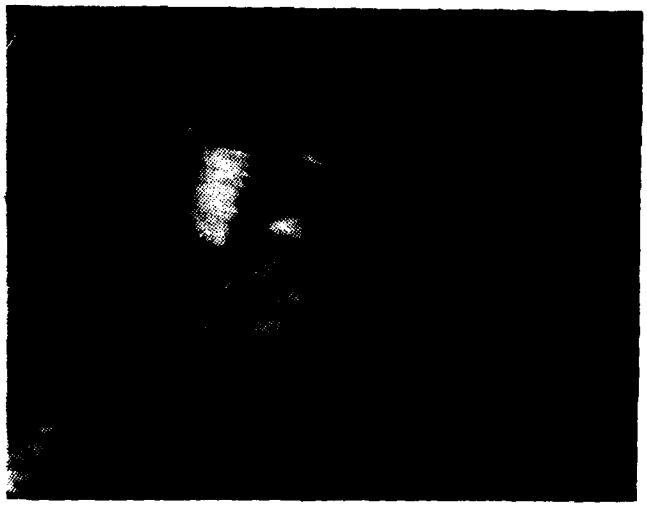

Micrograph 4. Alloy D. Martensitic plate with a minute change in habit plane occurring soon after nucleation. x14,000

Micrograph 5. Alloy D. Martensite plates originating from an array of lattice defects, which may possibly serve as preferred nucleation sites. x12,500

Micrograph 6. Alloy D, annealed and quenched, after 20 complete thermal cycles. This dislocation substructure is formed as a result of the transformations brought on by thermal cycling. x27,000

Micrograph 7. Alloy D, annealed and quenched, after 20 thermal cycles. This is the same region seen in Micrograph 6. Dislocations are observed both forming a substructure and as individual defects in the matrix. x10,000

Micrograph 8. Alloy D, annealed and quenched, after 20 thermal cycles. Dislocation arrays formed during thermal transformation cycling. x27,000

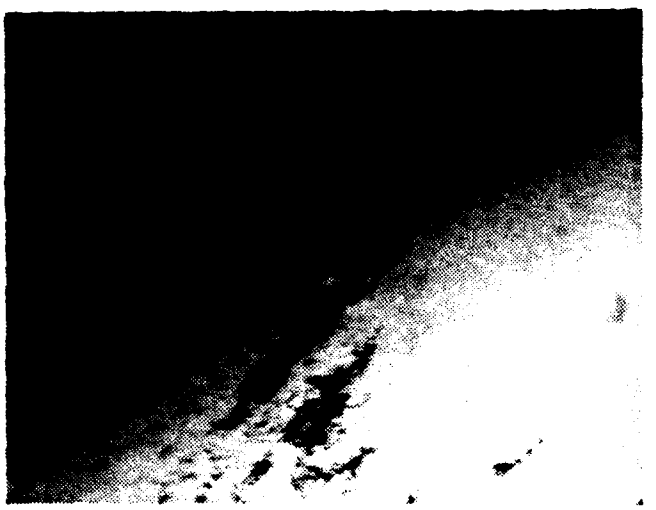

Micrograph 9. Alloy D annealed and quenched, after 20 thermal cycles. Dislocation substructure formed during thermal transformation cycling. x12,500

Micrograph 10. Alloy D annealed and quenched, after 20 thermal cycles. Dislocations generated during the martensitic transformations are observed to congregate in the parent matrix. x10,000

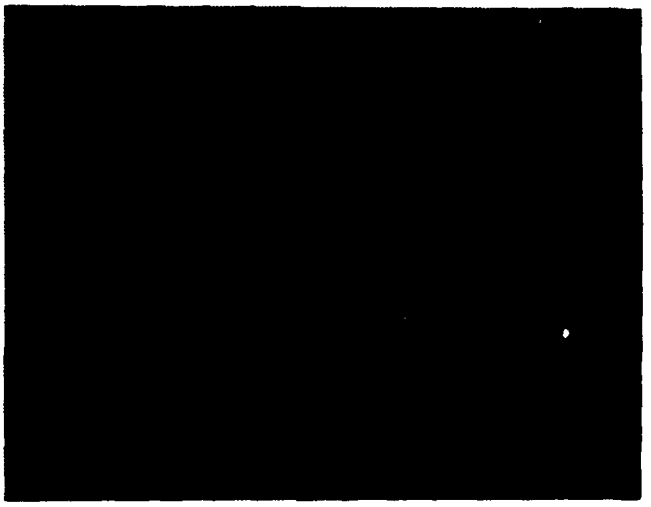

Micrograph 11. Alloy D annealed and quenched, after 20 thermal cycles. Dislocations arrayed on parallel slip planes. x30,000

Micrograph 12. Alloy D annealed and quenched, after 20 thermal cycles. Several dislocations are seen to stack up on similar slip planes. x10,000

Micrograph 13. Alloy D annealed and quenched, after 20 thermal cycles. Dislocations highlighted on a contour line, are stacked up on parallel slip planes. x11,000

Micrograph 14. Alloy D annealed and quenched, after 20 thermal cycles. Martensite plates, likely generated by electropolishing are observed to exist on parallel planes. x30,000

Micrograph 15. Alloy D annealed, quenched and rolled to about 90% of original thickness. A disarray of martensite plates and dense dislocation structure are present with the parent phase. x30,000

Micrograph 16. Alloy D annealed, quenched and rolled to approximately 90% of original thickness. A fairly large region of beta phase, containing a high dislocation density, is observed here. x18,000

Micrograph 17. Alloy D annealed, quenched and rolled to approximately 90% of original thickness. Martensite plates in early stages of growth are seen forming against a background characteristically caused by severe deformation. x16,000

Micrograph 18. Alloy D annealed, quenched and rolled to approximately 90% of original thickness. Martensite is observed forming at different orientations. x10,000

Micrograph 19. Alloy D annealed, quenched and rolled to about 90% of original thickness. Martensite is seen to be branching out into the matrix from an existing martensite plate. Note the similar orientation of the martensite branches. x8,000

Micrograph 20. Alloy D annealed, quenched and rolled to approximately 90% of original area. The martensite plates are separated by regions of parent phase. x24,000

Micrograph 21. Alloy D annealed, quenched and rolled to approximately 90% of original thickness. This micrograph depicts the severe deformation and retained martensite resulting from cold working the beta phase. x34,000

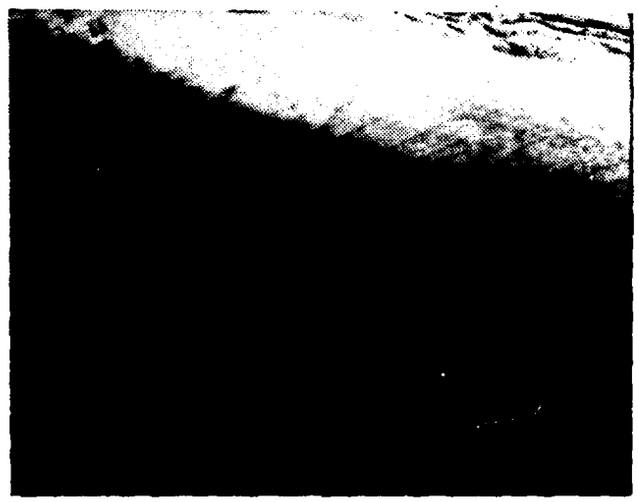

Micrograph 22. Alloy E annealed and quenched, prior to thermal cycling. Quenching alloy E from the beta phase is equivalent to one half a thermal cycle. Note the arrayed dislocations in this martensite plate. x15,000

Micrograph 23. Alloy E annealed and quenched, prior to thermal cycling. The martensite plates are observed to be faulted. x24,000

Micrograph 24. Alloy E annealed and quenched, prior to thermal cycling. The junction of several self-accommodating martensite plates in a plate group is seen here. x12,500

Micrograph 25. Alloy E annealed and quenched, prior to thermal cycling. This region of parent phase is adjacent to a martensitic plate. The dislocations were possibly generated as a result of the adjacent transformation during quenching. x12,500

Micrograph 26. Alloy E annealed, quenched and thermally cycled 20 times. Portions of alloy E are parent phase at room temperature. Here, a dislocation substructure is observed in this parent phase. x10,000

Micrograph 27. Alloy E annealed, quenched and thermally cycled 20 times. Parent phase and a martensite plate are seen in this micrograph. Judging from the lack of a dislocation substructure it is likely that this material is not transforming during thermal cycling. x14,000

Micrograph 28. Alloy E annealed, quenched and thermally cycled 20 times. Once again an absence of dislocations is noted in the parent phase after thermal cycling. x25,000

Micrograph 29. Alloy E annealed, quenched and thermally cycled 20 times. Some regions of existing parent phase do have dislocation substructures. x10,000

Micrograph 30. Alloy E annealed, quenched and thermally cycled 20 times. The structure of the parent phase is seen here highlighted by a contour line. x27,000

Micrograph 31. Alloy E annealed, quenched and thermally cycled 20 times. Dislocations, resulting from the martensitic transformations are outlined by a contour line. x12,500

Micrograph 32. Alloy D annealed, quenched and thermally cycled 20 times. The growth end of a martensite plate is observed blending into the matrix. x15,000

Micrograph 33. Alloy D annealed, quenched and thermally cycled. Dislocations, generated by martensitic transformations, are observed congregated in tangles. x15,000

Micrograph 34. Alloy D annealed, quenched and thermally cycled 20 times. A martensitic plate root, recognized by the changes in contour lines, is observed in the beta matrix. x12,500

APPENDIX

The specified transformation temperatures for alloys D and E are listed below. The data listed for alloy D is from the first complete thermal cycle. Data given for alloy E is from the second complete thermal cycle, since no peak was observed during the first half heating cycle.

	ALLOY D	ALLOY E
M_s	269	296
M_f	251	276
M_{max}	260	287
A_s	261	293
A_f	279	305
A_{max}	273	299

Calculations of the heats of transformation were based on the maximum area observed during thermal cycling. The borders of the area were estimated (as discussed under Experimental Procedures) and measured with a planimeter. The DSC constant was determined by cycling a standard sample (Indium) through fusion in the DSC.

$$H_t = \frac{K \times (\text{Range}) \times (\text{area})}{(\text{Chart Speed}) \times (\text{Sample Weight})}$$

$K = 2.86$ mm/(Area in. sq.)

H_t = Heat of transformation

ALLOY D $H_t = 2.497$ calories/gram

ALLOY E $H_t = .333$ calories/gram

LIST OF REFERENCES

1. Perkins, J., Thermomechanical Aspects of Shape Memory Alloys, paper presented at the Summer School on "Materials with Shape Memory," Jablonn, Poland, 29 June - 4 July 1981.

2. Pops, H. and Massalski, T. B., "Thermoelastic and Burst-Type Martensites in Copper-Zinc Beta-Phase Alloys," Transactions of the Metallurgical Society of AIME, Volume 230, pp. 1662-1668, December 1964.

3. Kajiwara, S., "New Aspects of Martensitic Transformations," supplement to Trans-Jap. Inst. Metals, 1976, Vol. 17, p. 81.

4. Guenin, G. and Gobin, P. F., A Localized Soft Model for the Nucleation of Thermoelastic Martensitic Transformation, unpublished.

5. Li, J. C. and Ansell, G. S., The Effect of Thermal Cycling on the Thermal Elastic Martensitic Transformation in Cu-Zn-Al Alloys, Rensselaer Polytechnic Inst., Troy, New York, to be published.

6. Hummel, R. E., Koger, J. W. and Pasupathi, U., "The Effect of Deformation on the Martensitic Transformation of Beta Brass," Transactions of the AIME, Vol. 242, pp. 249, February 1968.

7. Delaey, L., Perkins, A. J. and Massalski, T. B., "Review: on the Structure and Microstructure of Quenched Beta-Brass Type Alloys," Journal of Material Science, Vol. 7, pp. 1197-1215, 1972.

BIBLIOGRAPHY

Shape Memory Effect in Alloys, Perkins, J. ed., Plenum Press, New York, 1975.

INITIAL DISTRIBUTION LIST

		No. Copies
1.	Defense Technical Information Center Cameron Station Alexandria, Virginia 22314	2
2.	Library, Code 0142 Naval Postgraduate School Monterey, California 93940	2
3.	Department Chairman, Code 69 Department of Mechanical Engineering Naval Postgraduate School Monterey, California 93940	1
4.	Professor J. Perkins, Code 69Ps Department of Mechanical Engineering Naval Postgraduate School Monterey, California 93940	2
5.	LT William E. Muesing 7244 York Ave. S. #215 Edina, Minnesota 55435	1

END

DATE
FILMED

8 82

DTIC